

## Microscale simulation of resin-air flow around single fibers

Yasuhiro Inoue<sup>1\*</sup>, Michihito Matsumoto<sup>2</sup>, Masaki Hojo<sup>1</sup>, Kazuki Ishida<sup>1</sup>,  
Naoki Takada<sup>3</sup> and Taiji Adachi<sup>1</sup>

<sup>1</sup> *Kyoto University, Department of Mechanical Engineering and Science, Kyoto, Japan*

<sup>2</sup> *Advanced Technology R&D Center, Mitsubishi Electric Corp., Amagasaki, Japan*

<sup>3</sup> *National Institute of Advanced Industrial Science and Technology, Tsukuba, Japan*

**ABSTRACT:** We have developed a numerical code to implement a multiphase fluid model that employs the Navier–Stokes equation and includes the interfacial tension term and the Cahn–Hilliard equation for describing the resin-air interface. We perform preliminary numerical simulations of microscale resin-air flow around a regular lattice array of four single fibers. To investigate the effects of the resin-air interface on void formation, we numerically analyze four cases in which the longitudinal (i.e., along the flow direction) gap between two individual fibers is the same or twice the transverse gap with two different interfacial tension coefficients. From the analysis, we find that (1) the Laplace pressure due to the finite curvature of the resin-air interface can drive a transverse flow (capillary-driven flow) that penetrates into the longitudinal gap between the two fibers; (2) there is a dual time scale even at the microscale for determining the flow patterns: one of them is caused by the main flow and the other by capillary-driven transverse flow; and (3) voids are likely to form when the time scale of the main flow is shorter than that of the capillary flow. These results provide key factors for better understanding microvoid formation and to control it during the molding process.

**KEYWORDS:** numerical simulation, single-filament scale, multiphase flow, capillary effect, microvoid

### INTRODUCTION

Resin impregnation is an integrant of resin flow between the intramicropores inside fiber tows. On the intrapore scale, microscale factors such as shape, arrangement, and wettability can play a dominant role in determining the flow and the impregnation pressure gradient. In this study, we construct a numerical simulation code based on mathematical models that describe multiphase fluid flow on the microscale. Our approach differs from the previous studies because we explicitly take into account the resin-air interface and individual filaments, instead of treating them homogeneously. This approach allows us to investigate the manner in which microscale factors are related to microvoid generation.

### MATHEMATICAL MODEL

#### Resin-Air Fluid Model

To simulate resin-air flow on the scale of the individual filament, we adopt Takada's model [1] of multiphase fluids that is based on the phase-field Navier–Stokes (NS)

equation. We briefly introduce Takada's model. To describe each phase of the fluid, we introduce an order parameter  $\phi(x)$  and a free-energy functional  $\Psi$  as follows:

$$\Psi = \int d^3\mathbf{x} \left[ \psi(\phi(\mathbf{x}), T) + \frac{\kappa_f}{2} (\nabla \phi(\mathbf{x}))^2 \right], \quad (1)$$

where the first term on the right-hand side indicates the internal energy of the fluid and the second term indicates the energy penalty due to the inhomogeneity of the fluid. Here,  $\kappa_f$  is a model parameter that determines the width of the interface between two phases such as resin and air. In the current study, to numerically simulate the resin-air flows on the microscale instead of constructing a realistic model of  $\psi(\phi(\mathbf{x}), T)$ , we employ van der Waals model [2] for  $\psi(\phi(\mathbf{x}), T)$

$$\psi(\phi, T) = \phi \left\{ T \ln \left( \frac{\phi}{1 - B\phi} \right) - A\phi \right\}, \quad (2)$$

where  $A$  and  $B$  are the virial coefficients and represent attractive and repulsive molecular interactions, respectively. At an arbitrary temperature  $T$  that is less than the critical temperature  $T_c = 8A/27B$ , the two extreme values can be stable with respect to  $\phi$ , where one of them is  $\phi_{\max}$  and the other is  $\phi_{\min}$ . In this study, resin and air are represented by  $\phi_{\max}$  and  $\phi_{\min}$ , respectively.

Order-parameter dynamics can be described by the Cahn–Hilliard (CH) equation

$$\frac{\partial \phi}{\partial t} + \nabla \cdot (\phi \mathbf{u} + \mathbf{J}) = 0, \quad (3)$$

where  $\mathbf{u}$  indicates the convection velocity vector of the fluid flow and  $\mathbf{J}$  indicates the non-equilibrium flux vector of the order parameter

$$\mathbf{J} = -\Gamma \phi \nabla \mu, \quad (4)$$

$$\mu = \frac{\delta \Psi}{\delta \phi}. \quad (5)$$

To solve the Cahn–Hilliard equation [Eq. (3)] for  $\phi$ , we must know  $\mathbf{u}$  and  $\mathbf{J}$  in advance.  $\mathbf{J}$  can be calculated using Eq. (5);  $\mathbf{u}$  is given by the NS equation that describes the conservation of fluid momentum. We will explain the manner in which the CH and NS equations are coupled together.

### Filament-Fluid Interface Model

The contact angle defined by the resin-air, resin-filament, and filament-air interfaces plays a dominant role in determining the microscale multiphase flows. Because we introduce the free-energy functional to express multiphase fluids, the contact angle can be reproduced based on an effective interfacial energy between the resin and filament. Here, we introduce the effective interfacial energy as  $-\gamma_s \phi$  for simplicity. Thus, the boundary condition of the order parameter for the filament can be expressed as [3]

$$\mathbf{n} \cdot (\kappa_f \nabla \phi) = -\gamma_s \quad (6)$$

and the Neumann boundary condition should be also imposed to express the fact that the order parameter remains constant

$$\mathbf{n} \cdot \mathbf{J} = 0 \quad (7)$$

### Resin-Air Fluid Flow Model

To express multiphase flow, we introduce the mass-density continuity equation and the NS equation as follows:

$$\frac{\partial \rho}{\partial t} + \nabla \cdot \rho \mathbf{u} = 0, \quad (8)$$

$$\rho \frac{D\mathbf{u}}{Dt} = -\nabla \cdot \mathbf{P} + \nabla \left[ \eta \left\{ \nabla \mathbf{u} + (\nabla \mathbf{u})^T \right\} \right] + \mathbf{f}^{(k)}, \quad (9)$$

where  $\rho$  is the density of mass,  $\eta$  is the fluid viscosity, and the pressure tensor  $\mathbf{P}$  includes the pressure and interfacial stress as follows:

$$\mathbf{P} = \left[ p + \kappa_i (\nabla \rho)^2 \right] \mathbf{I} + \kappa_i \nabla \rho \otimes \nabla \rho. \quad (10)$$

Here, the interfacial tension  $\sigma$  between the resin and air is expressed by integration along the axis  $\xi$ , which is normal to the interface, as

$$\sigma = \kappa_i \int \left( \frac{\partial \rho}{\partial \xi} \right)^2 d\xi. \quad (11)$$

To convert the order-parameter field into the multiphase-fluid field, we introduce the following equations:

$$\rho = \begin{cases} \rho_R & \text{for } \phi \geq \phi_R \\ \frac{\rho_R + \rho_A}{2} + \frac{\rho_R - \rho_A}{2} \sin \left( \frac{\phi - (\phi_R + \phi_A)}{\phi_R - \phi_A} \right) & \text{for } \phi_A < \phi < \phi_R \\ \rho_A & \text{for } \phi \leq \phi_A \end{cases}, \quad (12)$$

$$\eta = \eta_A + \frac{\eta_R - \eta_A}{\rho_R - \rho_A} (\rho - \rho_R) \quad (13)$$

Here, we introduce two thresholds,  $\phi_R$  and  $\phi_A$ , to distinguish resin and air, respectively.

## SIMULATION

### Conditions

To simulate the flow dynamics of resin and air, we introduce the following simplified boundary conditions for filaments: (1) the filament has a square shape, (2) filaments are aligned in a rectangular arrangement, and (3) the resin-air, resin-filament, and filament-air interfaces contact orthogonally. Because this study constitutes the first simulation of the microscale resin-air flow around individual single filaments, we simplify the problem from the numerical and the physical point of view. Because we adopt the finite-difference method for both temporal and spatial differentiations, the space of the system is discretized by a square lattice. To eliminate the numerical error related to this discretization, we employ boundary conditions (1) and (2). The condition (3) is introduced to focus on the effect related to the balance between the interfacial tension of the resin-air and the pressure gradient of the resin. These simplifications will be made step-by-step in future study. We will be presenting few simulations under more realistic conditions in the current presentation.

Figure 1 shows a schematic representation of the simulation setup. The resin flow is driven along the negative  $y$  direction. Figure 1A (case 1) shows that the inter-filament space  $d_x$  along the  $x$  axis is equivalent to that along the  $y$  axis  $d_y$ , and Fig. 1B (case2) shows that  $d_y$  is half of  $d_x$ . The resin-air interfacial tension is set to one of the two values,  $\sigma \in \{0.15, 0.30\}$ . The impregnation pressure gradient is modeled as a constant driving force  $g$  along the  $y$  axis. Other parameter values are set as shown in Table 1. These parameter values lead to  $\text{Re} \approx O(1)$  and  $\text{Ca} \approx O(10^{-1})$ .

## Results

Snapshots of the simulation results of resin-air flows are displayed in Figs. 2–4, with the simulation conditions described in the figure captions. The visualization is based on the intermediate density  $\rho = 0.5$ .

## Discussion

On comparing Fig. 2 with Fig. 3, we observe the effects of the filament arrangement represented by  $d_y/d_x$ . For  $d_y/d_x = 1$ , transverse flows along the  $x$  axis into the interspaces between F1 and F2 and between F3 and F4 are observed; they are driven by capillary forces. Finally, the resin percolates into these interspaces by contacting two counter-flow fronts. However, for  $d_y/d_x = 0.5$ , the longitudinal-flow front reaches F2 and F4 before the transverse flow percolates into the interspaces between F1 and F2 or between F3 and F4. Thus, air is entrapped in the interspaces and there can be two time scales that are important in void generation: the time scale caused by transverse flow, and the time scale caused by longitudinal flow. If the longitudinal-flow time scale is shorter than the transverse-flow time scale, air is entrapped in the interspaces.

On comparing Fig. 2 with Fig. 4, we observe the effects of interfacial tension on void generation. As discussed previously, to avoid void generation, the transverse-flow time scale should be shorter than the longitudinal-flow time scale. However, because the interfacial tension used in Fig. 4 is the half of that used in Fig. 2, the velocity of the longitudinal-flow front in Fig. 4 is greater than that in Fig. 2. Thus, because the longitudinal-flow time scale becomes shorter, air is entrapped at the back steps of F1 and F3 while the transverse flows are being driven by capillary forces into the interspaces between F1 and F2 and between F3 and F4. In this study, the entrapped air is stably fixed to the filament in the back-step flow. It is necessary to know the critical shear stress and the contact angle to eliminate the entrapped air from the filament, such as, for studies on bubbles in shear flow [4, 5]; however, this is beyond the scope of the current study.

## CONCLUDING REMARKS

We have developed a numerical code to simulate resin-air flow on the scale of individual filaments, and have applied it to investigate the effects of filament arrangement and interfacial tension at the resin-air interface. In our simulations, microvoid generation is reproduced. Our results suggest that the relative magnitude of the two time scales determined by transverse and longitudinal flow is important in void generation. In the future study, we will expand the mathematical model to take into account more realistic conditions, such as, the circular shape of filaments and three-dimensional arrangements.

## REFERENCES

- [1]N. Takada, J. Matsumoto, S Matsumoto, N. Ichikawa: J. Comput. Sci. Technol. 2, (2008), 318-329.
- [2]F. Reif: Fundamentals of Statistical and Thermal Physics, McGraw-Hill, Inc. (1965), p. 173.
- [3]D. Jacqmin: J. Comput. Phys. 155, (1999), 96-127.
- [4]R. G. Cox: J. Fluid Mech. 37, (1969), 601-623.
- [5]J. M. Rallison: Ann. Rev. Fluid Mech. 16, (1984), 45-66.

## Tables and Figures

Table 1: Parameters

Parameter	$\rho_R$	$\rho_A$	$\eta_R$	$\eta_A$	$\kappa_f$	$\Gamma$	$g$
Value	1.0	$1.247 \times 10^{-3}$	0.5	$1.71 \times 10^{-3}$	0.1	12.0	$-1.0 \times 10^{-4}$

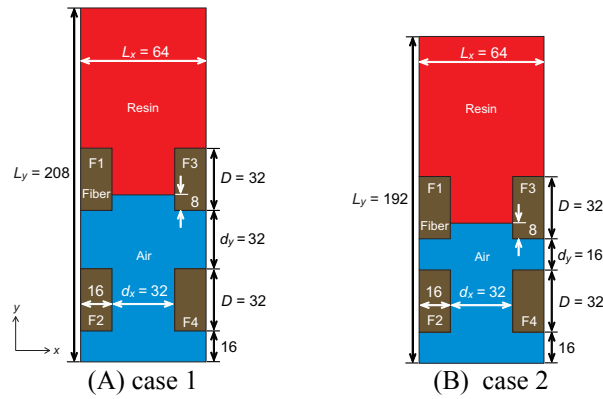


Fig.1 Schematic representation of simulation setup.

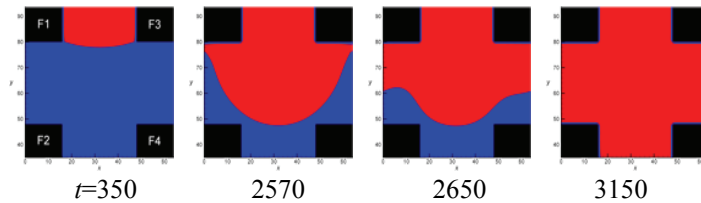


Fig.2 Snapshots of simulation results at time step  $t$ ,  $\sigma = 0.3$ , and  $d_y/d_x = 1$  (Case 1). Red and blue indicate resin and air, respectively.

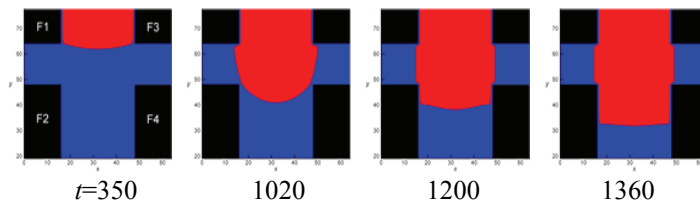


Fig.3 Snapshots of simulation results at time step  $t$ ,  $\sigma = 0.3$ , and  $d_y/d_x = 0.5$  (Case 2). Red and blue indicate resin and air, respectively.

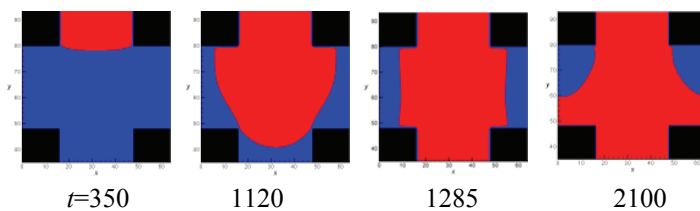


Fig.4 Snapshots of simulation results at time step  $t$ ,  $\sigma = 0.15$ , and  $d_y/d_x = 1$  (Case 1). Red and blue indicate resin and air, respectively.